Technical Report: Evaluation of peripheral dose for flattening filter free photon beams

E.L. Covington[1], T.A. Ritter[1,2], J.M. Moran[1], A.M. Owrangi[1], and J.I. Prisciandaro[1]

[1] *Department of Radiation Oncology, University of Michigan, Ann Arbor, MI 48109*

[2] *Department of Radiation Oncology, Veterans Affairs Ann Arbor Healthcare System, Ann Arbor, MI 48105*

Purpose: To develop a comprehensive peripheral dose (PD) dataset for two unflattened beams of nominal energy 6 and 10 MV for use in clinical care.

Methods: Measurements were made in a 40 x 120 x 20 cm^3 (width x length x depth) stack of solid water using an ionization chamber at varying depths (dmax, 5 cm, and 10 cm), field sizes (3 x 3 to 30 x 30 cm^2), and distances from the field edge (5 cm to 40 cm). The effects of the multileaf collimator (MLC) and collimator rotation were also evaluated for a 10 x 10 cm^2 field. Using the same phantom geometry, the accuracy of the anisotropic algorithm (AAA) and Acuros dose calculation algorithms were assessed and compared to measured values.

Results: The PD for both the 6 FFF and 10 FFF photon beams were found to decrease with increasing distance from the radiation field edge and decreasing field size. The measured PD was observed to be higher for the 6 FFF than for the 10 FFF for all field sizes and depths. The impact of collimator rotation was not found to be clinically significant when used in conjunction with MLCs. AAA and Acuros algorithms both underestimated the PD with average errors of -13.6% and -7.8%, respectively, for all field sizes and depths at distances of 5 and 10 cm from the field edge, but the average error was found to increase to nearly -69% at greater distances.

Conclusions: Given the known inaccuracies of peripheral dose calculations, this comprehensive dataset can be used to estimate out of field dose to regions of interest such as organs at risk, electronic implantable devices, and a fetus. While the impact of collimator rotation was not found to significantly decrease PD when used in conjunction with MLCs, results are expected to be machine model and beam energy dependent. It is not recommended to use a TPS to estimate PD due to the underestimation of out of field dose and the inability to calculate dose at extended distances due to limits of the dose calculation matrix.

Key words: Peripheral dose, out-of-field dose, flattening filter free, unflattened beams

1. INTRODUCTION

As the clinical use of flattening filter free (FFF) photon beams increases in radiation therapy, the need for in-depth characterizations of FFF beams has arisen due to inherent differences in beam properties from conventional flattened beams. The reported benefits of unflattened compared to flattened photon beams include an increase in dose rate, reduced scatter and leakage radiation, and a reduction in peripheral dose (PD).[1-11] Peripheral or out-of-field dose is defined as the absorbed dose outside of the radiation treatment field borders.[12, 13] Peripheral dose is due to contributions from leakage radiation from the head of the treatment unit, scatter radiation from the collimator head and beam modifiers, and internal scatter within the patient.[14-16] The PD may be clinically significant when dose to the fetus or to organs with low dose tolerances such as gonads, lens of eye must be minimized. Peripheral doses are also relevant when considering the risk of secondary malignancies or the potential failure of implanted electronic devices (e.g., pacemakers, defibrillators).[5, 12, 15, 17-19]

Numerous studies have investigated the trends in PD for flattened photon beams with varying field sizes, depth, and distances from the field edge, as well as the effects of beam modifiers (e.g., multileaf collimators [MLCs]) and collimator rotation.[12, 14-16, 20-24] The removal of the flattening filter changes the profile and dosimetric characteristics of photon beams.[3] As such, one cannot assume that the PD trends observed with flattened beams will be consistent with unflattened beams. Due to known inaccuracies of PD calculations with commercial treatment planning systems (TPSs),[18, 25] the typical means of assessing PD are through phantom measurements or Monte Carlo (MC) simulations.[4, 6]

Several MC publications[2, 5, 7, 9] have investigated PD of unflattened photon beams compared to flattened beams, both in the scenario in which the incident electron energy of the flattened and unflattened beams are matched (i.e., similar to the model utilized by Varian Medical Systems[10]), and when the incident energy of the unflattened beam is increased to match the attenuation of the corresponding flattened beam (i.e., similar to the model employed by Elekta[10]). The majority of these publications[2, 7, 9] have suggested that the PD of unflattened beams are lower than the corresponding PD for flattened beams, and that this difference increases with photon energy and decreasing field

size. Additionally, Almberg *et al.*[7] simulated both 6 FFF scenarios (incident electron energies of 6.45 and 8 MeV), and reported that the PD reduction was enhanced by increasing the incident photon energy (i.e., 8 MeV), suggesting that PD is not only dependent on the machine design but also on the implementation of the FFF technology. In contrast to previously published MC simulations, Kry *et al.*[5] reported that the difference in PD between flattened and unflattened photon beams is dependent on the distance from the field edge. Within the first 3 cm of the field, they observed that the PD of the FFF beam was lower than the corresponding flattened beam. At distances between 3 and 15 cm from the field edge, the PD was typically higher in FFF mode, and beyond 15 cm, the PD was again lower in FFF mode.

Also, PD of FFF beams has been studied for treatment plans generated for intensity modulated radiation therapy [IMRT], stereotactic body radiotherapy [SBRT], stereotactic radiosurgery [SRS][4, 8] as well as for square and rectangular open fields.[7, 11, 19] Similar to the MC studies, these publications have suggested that the PD of unflattened beams is lower than flattened beams of the same nominal energy, and that the relative difference in PD increases with energy.

The intention of the current study was to develop a comprehensive PD dataset for 6 FFF and 10 FFF photon beams that could be used for scenarios where the PD may be clinically relevant. We also compared the trends in PD measurements between the two unflattened beams, as well as compared the PD of the 6 FFF beam with the published results of a 6 MV flattened beam.[26]

2. METHODS

All measurements were performed for the 6 and 10 MV unflattened photon beams of a Varian TrueBeam linac (Varian Medical Systems, Palo Alto, CA) running version 1.6 of the control software and equipped with the Millennium 120-leaf multileaf collimators (MLCs). The PD of the two unflattened beams was determined with a 40 x 120 x 20 cm^3 (width x length x depth) stack of solid water (Solid Water model 457, Gammex/RMI, Milwaukee, WI) with an Exradin A12 ionization chamber (Standard Imaging, Middleton, WI) inserted in a 2 cm slab of solid water when positioned on the treatment couch (see Figure 1). Measurements were acquired at various depths (nominal depth of maximum dose, dmax [1.5 cm for the 6 FFF beam and 2.0 cm for the 10 FFF beam], 5 cm, and 10

cm), field sizes (3 x 3, 6 x 6, 10 x 10, 15 x 15, 20 x 20, 25 x 25, and 30 x 30 cm^2), and distances (5, 10, 15, 20, 30 and 40 cm) between the field edge and the center of the ionization chamber. The field aperture was shaped by matching the MLCs and the jaws, and a 90° collimator rotation was used. The distance from the field edge was defined at the surface of the solid water phantom where the source-to-surface distance was 100 cm (see Figure 1). Peripheral dose measurements were normalized to the measured central axis (CAX) dose at the nominal dmax for a given field size. Additionally, the effects of the tertiary MLC and collimator rotation were evaluated for a 10 x 10 cm^2 field size by acquiring PD measurements with the collimator positioned at both 0° and 90° for field aperture set with the collimator jaw and/or MLCs.

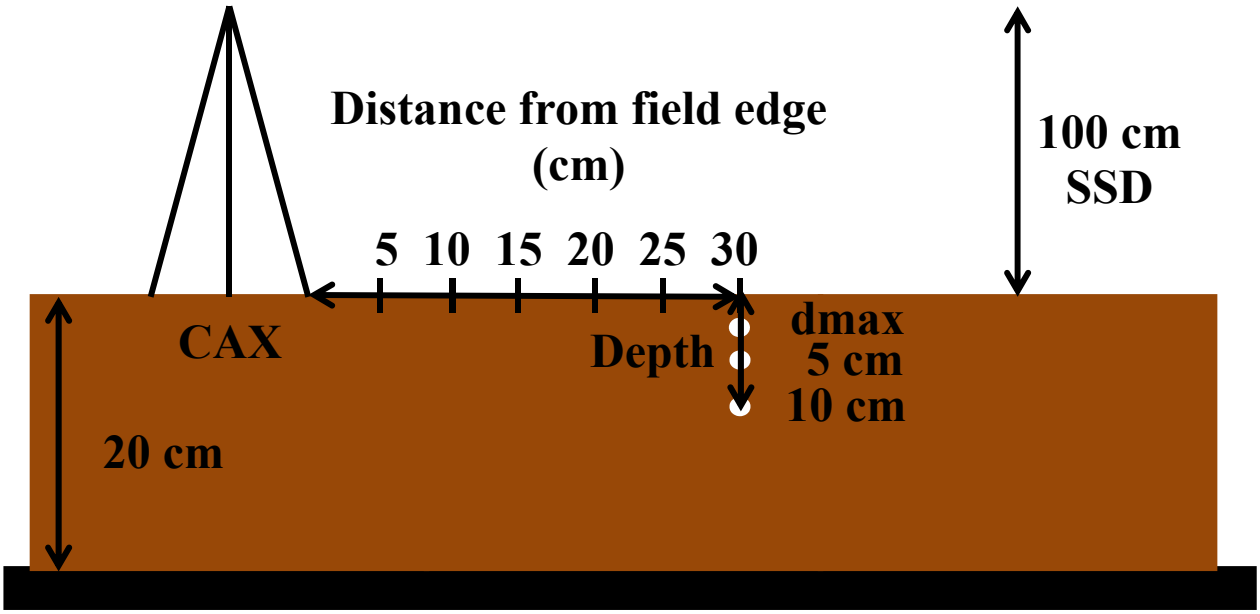

Figure 1. Schematic of the 40 x 120 x 20 cm^3 (width x length x depth) solid water phantom used for the PD measurements. The distances from the field edge were defined at a 100 cm source-to-surface distance (SSD). The schematic shows the three depths (nominal depth of maximum depth, dmax, 5 cm, and 10 cm) at which the ionization chamber was positioned in the solid water for the example of a 30 cm distance from the field edge.

To compare the measured PD with the dose calculated in the treatment planning system (TPS), a phantom with the same dimensions as the measurement phantom was generated in Eclipse (version 10, Varian Medical Systems, Palo Alto, CA). Beam models for the 6 FFF and 10 FFF were developed using the Varian Truebeam Representative Data

Set which was based on the average of three machines.[27] A series of treatment plans were created using a single anterior beam corresponding to each of the measured, static field sizes with a 90° collimator rotation. To calculate the PDs, reference points were added at the same depths and distances from the field sizes that were measured. The PDs were calculated using both the analytic anisotropic algorithm (AAA) version 10.0.42 and the Acuros XB (AXB) algorithm version 10.0.42 with a 0.25 cm grid size. The calculated PD was normalized to CAX at a depth of dmax to compare the normalized PD of both AAA and Acuros to the measured data.

3. RESULTS

The trends in the measured PDs for the 6 FFF and 10 FFF photon beams are shown in Figure 2. The PD for all field sizes (3 x 3 through 30 x 30 cm^2), and distances (5 - 40 cm) are shown in Table 1 for the 6 FFF beam and Table 2 for the 10 FFF beam.

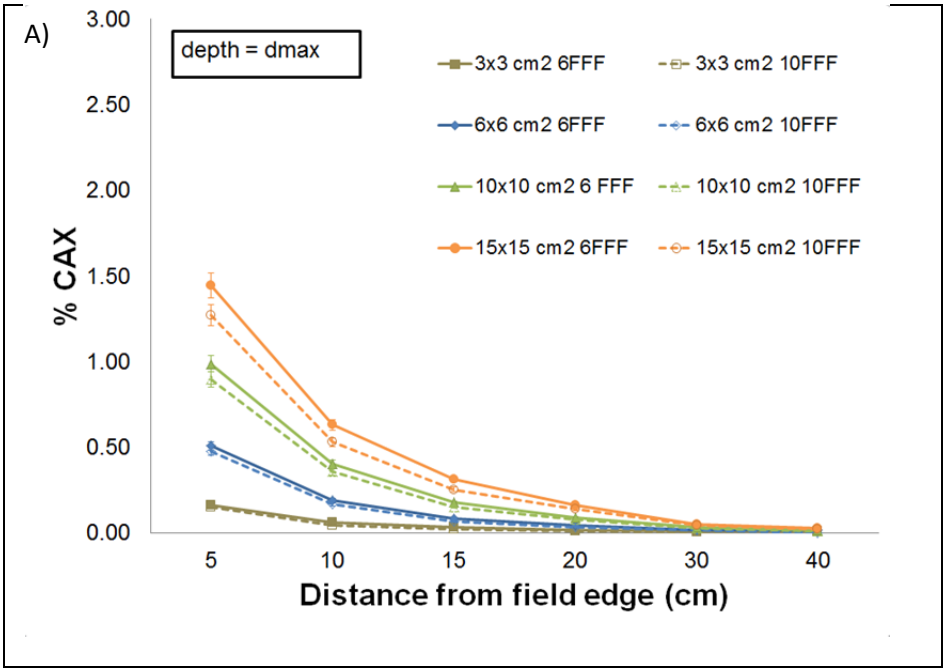

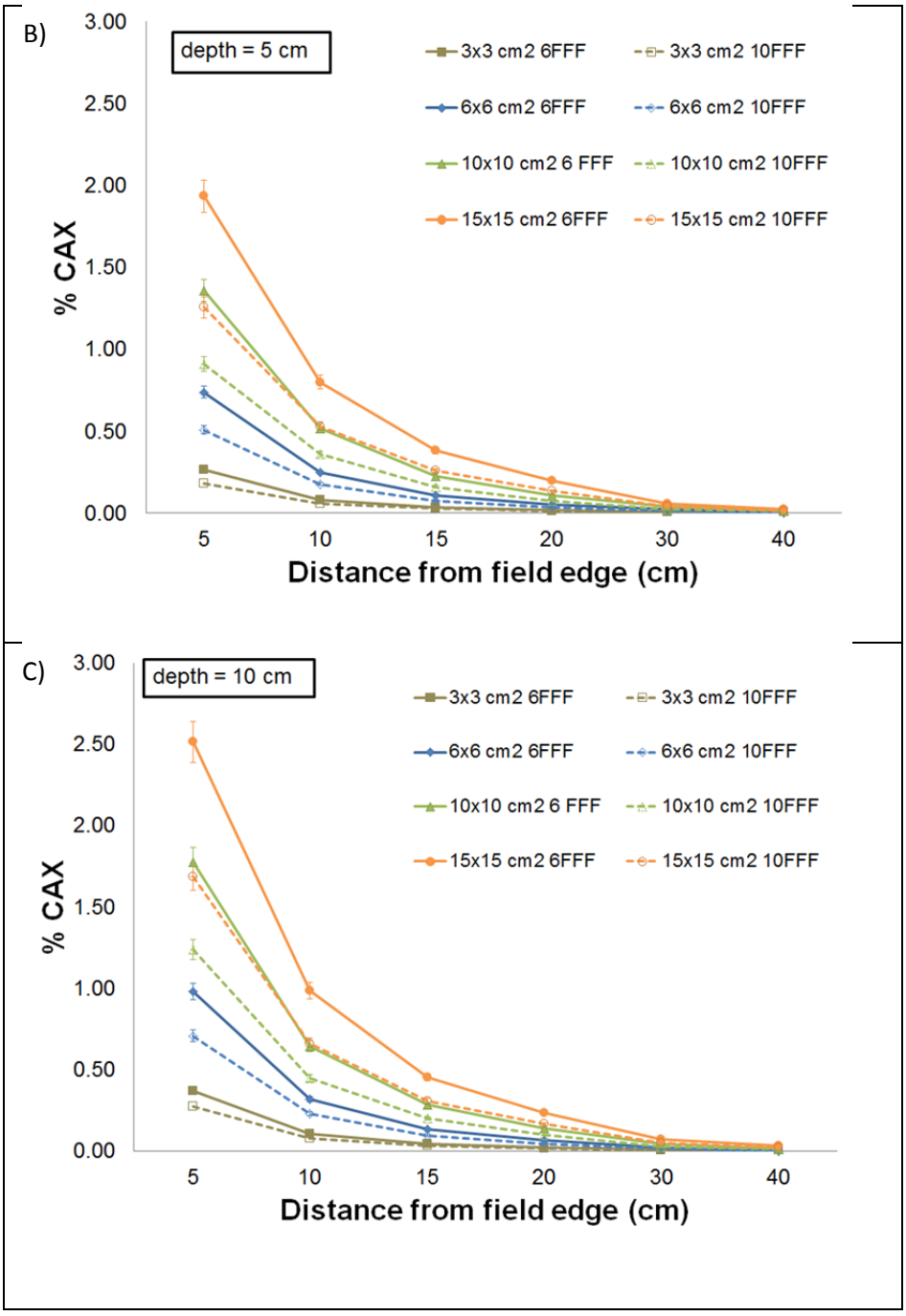

Figure 2. Measured PDs normalized to the central axis (CAX) dose at a depth of nominal dmax for the 6 FFF (solid line) and 10 FFF (dashed line) beams. The PD measurements are shown at a depth of A) nominal dmax (1.5 cm for the 6 FFF beam and 2.0 cm for the 10 FFF beam), B) 5 cm, and C) 10 cm, and were acquired for field sizes ranging from 3 x 3 to 30 x 30 cm^2, and distances of 5 to 40 cm from the field edge with the MLC shaping the field apertures and with a collimator rotation of 90°.

The measured PD at the nominal depth of dmax and at a distance of 5 cm from the field edge for a 6 x 6 cm^2 square field was 0.51% and 0.48% for the 6 FFF and 10 FFF photon beams, respectively. This compares to the measured PD for a 30 x 30 cm^2 field at the same depth and distance from the field edge of 2.01% and 1.63% for the 6 FFF and 10 FFF photon beams, respectively. The measured PD for the 6 x 6 cm^2 square field at a distance of 5 cm from the field edge was found to increase from 0.51% to 0.98% and 0.48% to 0.71% when the depth was varied between dmax and 10 cm, for the 6 FFF and 10 FFF photon beams, respectively.

Table 1. Percent ratio of the measured PD to the central axis (CAX) dose at a depth of 1.5 cm for varying field sizes and depths at distances ranging from 5 to 40 cm from the field edge for a 6 FFF photon beam.

				Distance from the field edge (cm)					
Field size (cm)	Depth (cm)	MLC status	Collimator Angle (degree)	5	10	15	20	30	40
3x3	1.5	Shaped	90	0.16	0.06	0.03	0.02	0.01	0.01
3x3	5	Shaped	90	0.26	0.08	0.04	0.02	0.01	0.01
3x3	10	Shaped	90	0.37	0.11	0.05	0.02	0.01	0.01
6x6	1.5	Shaped	90	0.51	0.19	0.08	0.05	0.02	0.01
6x6	5	Shaped	90	0.74	0.25	0.11	0.05	0.02	0.01
6x6	10	Shaped	90	0.98	0.32	0.13	0.06	0.23	0.00
10x10	1.5	Retracted	0	1.31	0.65	0.41	0.23	0.09	0.04
10x10	5	Retracted	0	1.62	0.71	0.41	0.22	0.10	0.04
10x10	10	Retracted	0	1.98	0.79	0.42	0.22	0.09	0.04
10x10	1.5	Retracted	90	1.22	0.61	0.34	0.15	0.07	0.03
10x10	5	Retracted	90	1.56	0.69	0.37	0.17	0.07	0.03
10x10	10	Retracted	90	1.96	0.78	0.40	0.18	0.07	0.03
10x10	1.5	Shaped	0	0.96	0.36	0.18	0.10	0.04	0.02

10x10	5	Shaped	0	1.33	0.48	0.22	0.12	0.04	0.02
10x10	10	Shaped	0	1.75	0.61	0.27	0.14	0.04	0.02
10x10	1.5	Shaped	90	0.99	0.41	0.18	0.09	0.04	0.02
10x10	5	Shaped	90	1.36	0.52	0.23	0.11	0.04	0.02
10x10	10	Shaped	90	1.78	0.64	0.28	0.14	0.04	0.02
15x15	1.5	Shaped	90	1.45	0.63	0.31	0.16	0.05	0.03
15x15	5	Shaped	90	1.93	0.80	0.38	0.20	0.06	0.03
15x15	10	Shaped	90	2.51	0.99	0.45	0.23	0.07	0.03
20x20	1.5	Shaped	90	1.74	0.79	0.39	0.23	0.07	0.03
20x20	5	Shaped	90	2.32	1.01	0.49	0.27	0.09	0.03
20x20	10	Shaped	90	3.01	1.23	0.58	0.30	0.10	0.04
25x25	1.5	Shaped	90	1.89	0.88	0.44	0.25	0.10	0.04
25x25	5	Shaped	90	2.54	1.13	0.56	0.30	0.11	0.05
25x25	10	Shaped	90	3.31	1.39	0.67	0.35	0.12	0.05
30x30	1.5	Shaped	90	2.01	0.95	0.48	0.28	0.12	0.05
30x30	5	Shaped	90	2.69	1.22	0.61	0.34	0.13	0.06
30x30	10	Shaped	90	3.52	1.50	0.74	0.39	0.13	0.06

Table 2. Percent ratio of the measured PD to the central axis (CAX) dose at a depth of 2 cm for varying field sizes and depths at distances ranging from 5 to 40 cm from the field edge for a 10 FFF photon beam.

Field size (cm)	Depth (cm)	MLC status	Collimator Angle (degree)	Distance from the field edge (cm)					
				5	10	15	20	30	40
3x3	2	Shaped	90	0.15	0.05	0.02	0.01	0.01	0.01
3x3	5	Shaped	90	0.18	0.06	0.03	0.01	0.01	0.01
3x3	10	Shaped	90	0.27	0.08	0.03	0.02	0.01	0.01
6x6	2	Shaped	90	0.48	0.17	0.07	0.03	0.02	0.00
6x6	5	Shaped	90	0.51	0.18	0.08	0.04	0.01	0.00
6x6	10	Shaped	90	0.71	0.23	0.09	0.04	0.02	0.00
10x10	2	Retracted	0	1.32	0.66	0.40	0.23	0.09	0.03
10x10	5	Retracted	0	1.17	0.54	0.33	0.18	0.08	0.03
10x10	10	Retracted	0	1.44	0.59	0.33	0.17	0.08	0.03
10x10	2	Retracted	90	1.15	0.55	0.32	0.14	0.06	0.03
10x10	5	Retracted	90	1.11	0.52	0.30	0.13	0.05	0.02
10x10	10	Retracted	90	1.41	0.58	0.31	0.13	0.05	0.02
10x10	2	Shaped	0	0.87	0.29	0.14	0.08	0.03	0.02
10x10	5	Shaped	0	0.90	0.32	0.15	0.08	0.03	0.02
10x10	10	Shaped	0	1.22	0.42	0.19	0.10	0.03	0.02
10x10	2	Shaped	90	0.90	0.36	0.15	0.08	0.03	0.01
10x10	5	Shaped	90	0.91	0.36	0.16	0.08	0.03	0.01
10x10	10	Shaped	90	1.24	0.45	0.20	0.10	0.03	0.01
15x15	2	Shaped	90	1.27	0.53	0.25	0.14	0.04	0.02
15x15	5	Shaped	90	1.26	0.53	0.26	0.14	0.04	0.02
15x15	10	Shaped	90	1.68	0.66	0.31	0.16	0.05	0.02
20x20	2	Shaped	90	1.49	0.64	0.31	0.18	0.06	0.03

20x20	5	Shaped	90	1.46	0.65	0.32	0.18	0.06	0.03
20x20	10	Shaped	90	1.95	0.80	0.38	0.20	0.07	0.03
25x25	2	Shaped	90	1.57	0.68	0.33	0.19	0.08	0.03
25x25	5	Shaped	90	1.56	0.71	0.36	0.20	0.08	0.03
25x25	10	Shaped	90	2.10	0.88	0.43	0.23	0.08	0.04
30x30	2	Shaped	90	1.63	0.72	0.35	0.21	0.09	0.04
30x30	5	Shaped	90	1.63	0.75	0.39	0.22	0.09	0.04
30x30	10	Shaped	90	2.18	0.93	0.46	0.25	0.09	0.05

The effect of a 0^o versus 90^o collimator rotation, as well as the impact of a tertiary MLC was also investigated for a 10 x 10 cm^2 field size. The difference in PD at depths of dmax, 5 and 10 cm for both 0° and 90° collimator rotation and MLC shaped field are shown in Figure 3 for both 6 FFF and 10 FFF beams. At a distance of 5 cm from the field edge and a depth of 1.5 cm, the measured PD for the 6 FFF beam was 1.31% versus 1.22% for the 0^o and 90^o collimator rotations. At the same distance from the field edge and a depth of 2 cm, the measured PD for the 10 FFF beam was 1.32% versus 1.15% for the 0^o and 90^o collimator rotations. The PD measured at the nominal dmax at 10 cm from the field edge was 0.36% versus 0.41% for the 6 FFF beam and 0.29% versus 0.36% for the 10 FFF beam for the 0^o and 90^o collimator rotations, respectively.

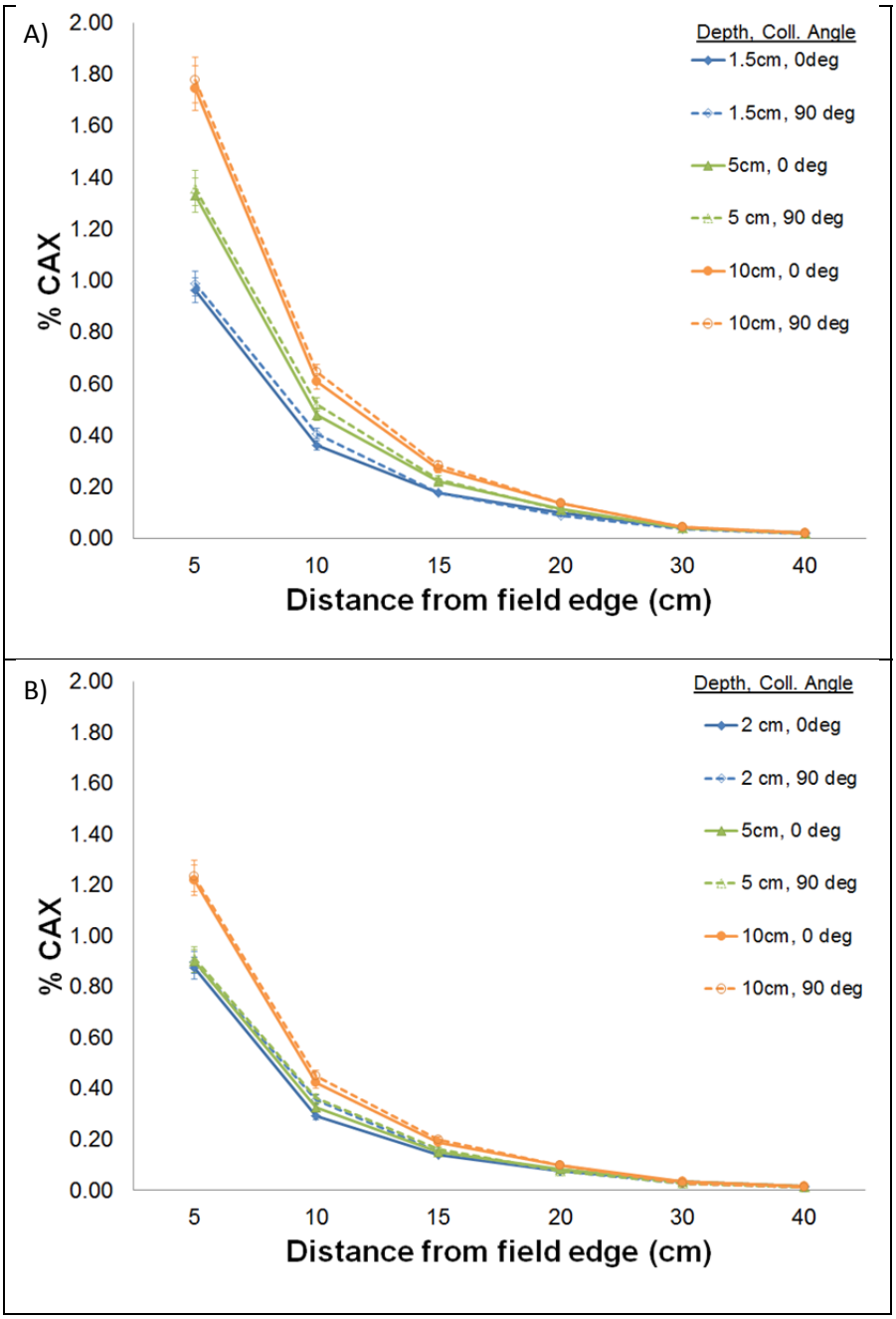

Figure 3. To evaluate the effects of collimator rotation (0^o – solid line and 90^o – dashed line) with the presence of the MLC, the measured PDs normalized to the central axis (CAX) dose at a depth of dmax is shown for A) 6 FFF and B) 10 FFF photon beams at depths of dmax, 5 cm, and 10 cm for both beam energies.

140

PD measurements for the 6 FFF beam were also compared to previously acquired PD measurements of a 6 MV beam on a Varian Trilogy linac (Varian Medical Systems, Palo Alto, CA).[26] Figure 4 shows the measured PDs normalized to the CAX at a depth of 1.5 cm for the 6 FFF and 6 MV beams which were acquired at depths of 1.5, 5 cm, 10 cm. The PD measurements are shown for field sizes ranging from 6 x 6 to 30 x 30 cm^2, and distances of 5 to 40 cm from the field edge with the MLC shaping the field apertures and with a collimator rotation of 90°. For larger field sizes (20 x 20 – 30 x 30 cm^2), the measured PD was smaller for the 6 FFF beam compared to the 6 MV beam, 2.01% compared to 2.57% for the 6 FFF and 6 MV photon beams, respectively, at a distance of 5 cm from the field edge for a 30 x 30 cm^2 square field. At a depth of 10 cm, the PD for the 6 FFF and 6 MV photon beams are nearly identical for the 6 x 6 and 10 x 10 cm^2 for all distances from the field edge. Similar results were seen for the 15 x 15 cm^2 for all distances from field edge except 5 cm, where the measured PD is 2.51% compared to 2.96% for the 6 FFF and 6 MV beams, respectively. For the larger field sizes (20 x 20 – 30 x 30 cm^2), the measured PD was smaller for the 6 FFF beam compared to the 6 MV beam, 3.52% compared to 5.56% for the 6 FFF and 6 MV photon beams, respectively, at a distance of 5 cm from the field edge for a 30 x 30 cm^2 square field.

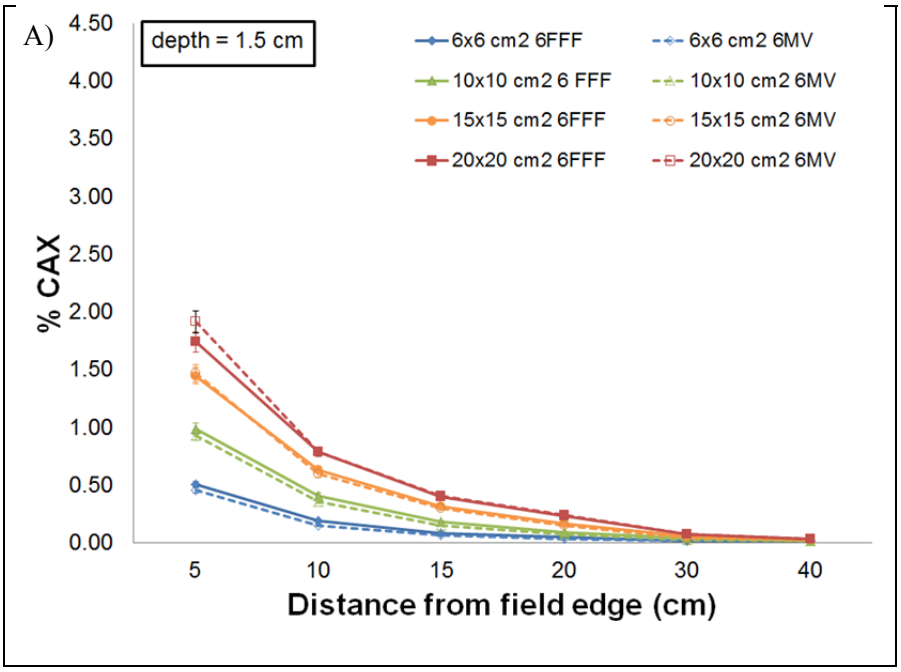

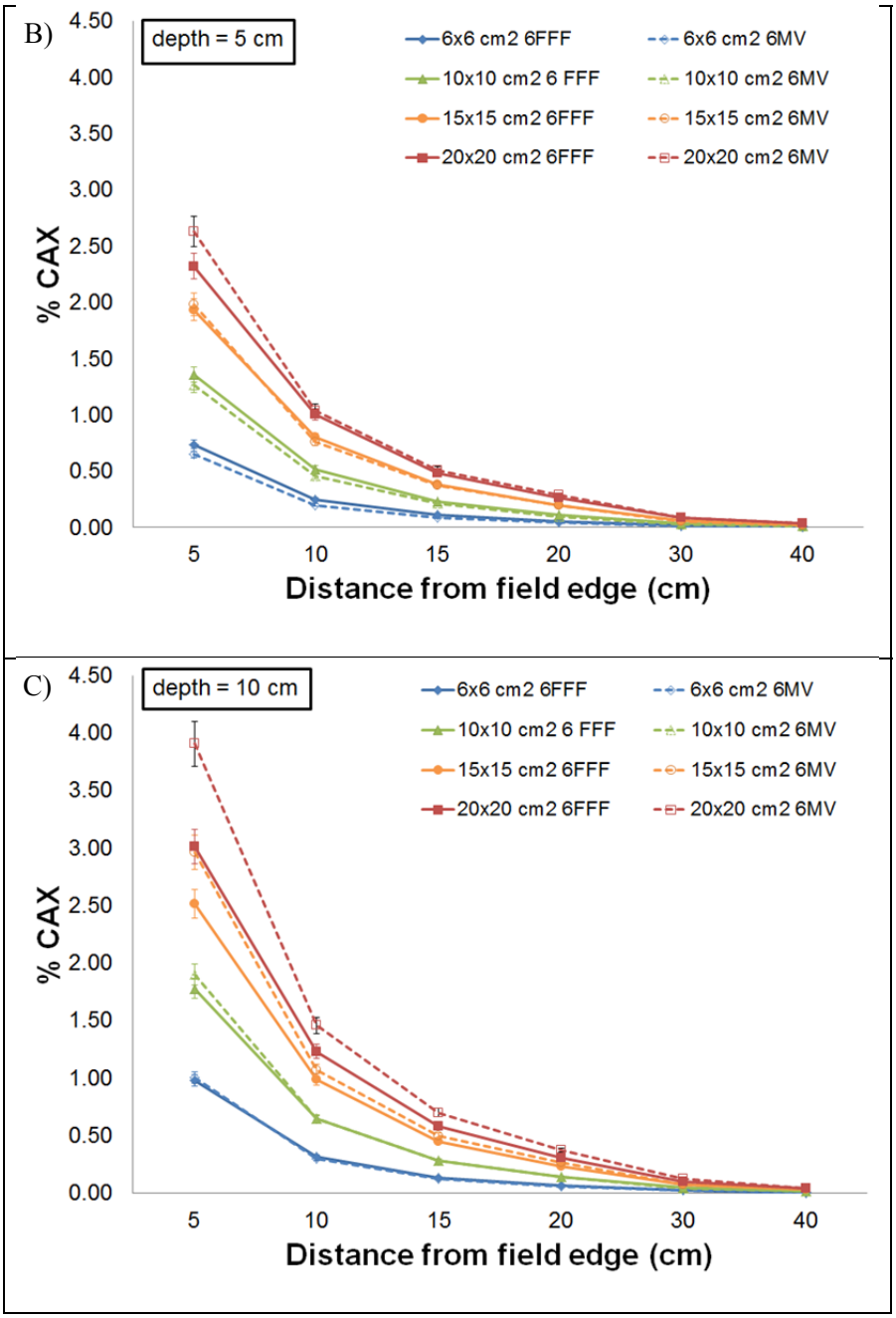

Figure 4. Measured PDs normalized to the central axis (CAX) dose at a depth of 1.5 cm for the 6 FFF (solid line) and 6 MV (dashed line) beams acquired at depths of A) 1.5 cm, B) 5 cm, and C) 10 cm. The PD measurements are shown for field sizes ranging from 6 x 6 to 30 x 30 cm^2, and distances of 5 to 40 cm from the field edge with the MLC shaping the field apertures and with a collimator rotation of 90°.

Peripheral dose was also modeled in Eclipse (version 10) using both the AAA and Acuros dose calculations models. Table 3 shows the percent error of the measured to calculated PD for 6 FFF and 10 FFF beams at 3x3 cm^2 and 6x6 cm^2 fields at depths of dmax, 5, and 10 cm. The difference in measured versus calculated dose has not been normalized to CAX dose and is therefore representative of the local rather than global error for AAA and Acuros. Between 5 and 10 cm from the field edge, the average percent error was found to be 9% and 9.3% for AAA and Acuros, respectively, at all energies and depths for 3x3 cm^2 and 6x6 cm^2 fields. For the field sizes (3 x 3 to 30 x 30 cm^2) evaluated, the average percent error was -13.6% for AAA and -7.8% for Acuros for all depths and distances of 5 and 10 cm from the field edge. At distances from the field edge of 15 cm and greater, AAA reported zero dose for all depths and field sizes. Acuros also reported zero dose at distances from the field edge of $\geq$ 15cm for field sizes $\geq$ 10x10 cm^2.

Table 3. Percent error of measured PD to calculated PD for both the AAA and Acuros dose calculation models for 3x3 and 6x6 cm^2 fields.

			% Error from Measurement					
			5 cm		10 cm		15 cm	
Energy (MV)	Field Size (cm^2)	Depth (cm)	AAA	Acuros	AAA	Acuros	AAA	Acuros
6 FFF	3 x 3	1.5	-1.2	-6.1	-30.5	-13.6	-	-68.8
		5	3.8	-6.8	-13.4	-12.2	-	-44.4
		10	7.3	-5.7	-2.9	-12.4	-	-32.6
	6 x 6	1.5	-11.4	-12.4	-27.9	-6.3	-	-28.0
		5	1.9	-1.1	-13.7	-8.8	-	-18.3
		10	10.8	3.0	-4.4	-0.3	-	-9.2
10 FFF	3 x 3	2	-10.0	-9.3	0.0	0.0	-	-50.0
		5	-8.2	-13.6	-19.6	-19.6	-	-60.7
		10	3.3	-8.4	-12.8	-26.9	-	-30.3
	6 x 6	2	-24.6	-12.4	-28.3	-7.8	-	-33.3
		5	-6.3	-9.6	-20.3	-19.8	-	-28.6
		10	2.7	-4.1	-9.3	-8.4	-	-18.1

4. DISCUSSION

To demonstrate how this dataset can be implemented clinically, the following simple example is provided. A patient with a pacemaker is scheduled to undergo radiotherapy for a lung lesion with an average field size of 6x6 cm^2 and a 6 FFF beam. The prescription dose of 60 Gy is to be delivered using a 6 field treatment plan that includes anterior-posterior (AP), posterior-anterior (PA) and four oblique treatment beams. A detailed estimate of PD to the pacemaker is requested by the treating physician. For each field, the following methodology is applied: 1) the dose at 1.5 cm depth along the center of the field is found from the treatment planning system, 2) the distance from the beam edge to the most proximal portion of the pacemaker is measured in the treatment planning system, 3) the depth of the pacemaker from the body surface at the closest edge of the treatment field is measured, and 4) the appropriate figures or tables are used to estimate the out-of-field dose to the device. Pacemaker depths less than 1.5 cm are treated as though they were at 1.5 cm, while depths greater than 10 cm are treated as though they were at 10 cm. These assumptions are consistent with the references for out-of-field dose from flattened beams and provide a conservative estimate. As an illustration, an estimate of PD is presented for only the AP field of the six field plan. The AP field size is 6x6 cm^2 with a 90° collimator rotation delivering a dose of 15 Gy at a 1.5 cm depth along the center of the field. If the pacemaker is 5 cm from the field edge and at a 1.0 cm depth, Table 1 can be used to estimate the out of field dose from the AP beam. A PD of 0.51% is found from the first row of the 6x6 cm^2 field data (indicating a 1.5 cm pacemaker depth) under the column marked "5" (indicating a 5 cm distance from the field edge). The total out-of-field dose from the AP field is calculated as 15 Gy × 0.0051 = 7.7 cGy. Each of the fields can be individually considered in this manner and the result summed and then reported to the requesting physician.

The PD for both the 6 FFF (see Table 1) and 10 FFF (see Table 2) photon beams were found to decrease with increasing distance from the radiation field edge and decreasing field size. Additionally, when comparing the PD measurements for the 6 FFF and 10 FFF beams, the PD was observed to decrease with increasing energy. Overall, the measured PD was observed to be higher for the 6 FFF than for the 10 FFF for all field sizes and depths. These differences became more pronounced with increasing depth and field sizes and for measurement distances closest to

the field edge. All PD values were acquired using static fields; therefore, use caution when estimating PD for modulated fields.

When the field aperture was set by the collimator jaws alone, the PD was observed to be moderately higher for a 0^o collimator rotation relative to 90^o for both the 6 FFF and 10 FFF photon beams. Conversely, when the field aperture is shaped by the MLC, the PD measured at 0^o and 90^o are nearly identical for both the 6 FFF and 10 FFF beams with the exception of measurements acquired at all depths for a distance of 10 cm from the field edge. At this distance from the field edge, the PD was observed to be slightly higher with a 90^o collimator rotation. For the Truebeam, a minimal difference in PD was observed between the two collimator rotation angles at distances between 5 and 30 cm from the field edge which is consistent with the 6 MV flattened beam results reported by Mutic et al[20]. The impact of collimator rotation on PD may be dependent on machine make, model, and beam energy used; therefore, these results should not be assumed to translate across all machines.[28]

When comparing the measured PD for the 6 FFF and 6 MV flattened photon beam, the relative PD was found to depend on the depth, field size, and distance from the field edge (see Figure 4). At a depth of 1.5 cm, the PD for the 6 FFF beam was marginally higher than the 6 MV beam for 6 x 6 and 10 x 10 cm^2 field sizes up to a distance of 20 cm from the field edge, measuring 0.51% versus 0.46% for the 6 FFF and 6 MV photon beams, respectively, for a 6 x 6 cm^2 open field. The PD of the 6 FFF and 6 MV beam were nearly identical for the 15 x 15 cm^2 field size at all measured distances from the field edge.

Since PD is a relative measurement, many uncertainties in the data (e.g. calibration factor) do not impact the accuracy of the values. Since the data was collected over several weeks, the largest source of error is expected to be the uncertainty of the set-up relative to previous measurements. To ameliorate this uncertainty, repeat measurements were performed over the various data collection sessions to verify reproducibility of the set-up as well as the stability of equipment (e.g. ion chamber, electrometer). Please note, a limitation of the current study is that a single measurement was acquired for many data points due to the large number of measurements (greater than 400) required to monitor the PD trends. As such, standard deviations were unable to be calculated. Repeat measurements were performed on a subset of the data to address reproducibility. From nearly 30 repeat measurements of various energy, field size and distances from the field edge, the average deviation from the initial measurement was less than 4%;. However, when PD is on the order of 0.01% or less of the CAX dose, the

uncertainty is dominated by the resolution of the electrometer. Pion for the ion chamber used was 1.012 at central axis under calibration conditions for the 10FFF beam. Compared to a conventional flattened beam, this represents an approximately 0.7% increase in Pion that could indeed contribute to measured error when values are normalized to central axis. Combining this error in quadrature with set-up error results in a combined error of 4.1%; therefore we have conservatively added 5% error bars to all data points.

Similar to previous studies[18,25], the PD calculated using both AAA and Acuros was typically found to underestimate the dose when compared to measured values. The difference in measured and calculated dose typically increased as the distance the from the field edge increased for both algorithms although exceptions were noted. For example, the percent error in the TPS calculated dose for a 10 FFF 6x6 cm^2 field at 5 cm from the field edge was -24.6%. The percent error decreased to -7.8% at 10 cm from the field edge. For small field sizes, where FFF beams are primarily advantageous (e.g. SBRT, SRS), the underestimate of the PD dose with AAA and Acuros was of a similar magnitude.

Comparisons between the commercial algorithms and measurements at distances greater than 10 cm from the field edge were not performed, since AAA reports zero dose for the designated points of interest that were beyond 10 cm from the field edge. AAA uses a divergent dose matrix where the width of the calculation matrix is dependent on jaw position. The default margin is 12 cm from the field but can range for 7-12 cm to limit the number of calculation points. Acuros uses the same margins for input fluences, but extends the entire dose calculation to the entire calculation volume[a]. Even so, at distance of 15 cm and greater, Acuros only reported calculated doses up to field sizes of 10x10 cm^2. Acuros also underestimated the PD at 15 cm from the field edge for both 6 FFF and 10 FFF beams at field sizes of 3x3 and 6x6 cm^2 with an average percent error of -35%. The maximum percent error (-68.8%) was observed with a 6 FFF energy at 15cm from a 3x3 cm^2 field at 1.5 cm depth. This level of uncertainty in calculated dose has clinical significance for estimating dose to out of field organs at risk (OARs). For example, when estimating the dose to a fetus using a 3x3cm^2 field at 1.5 cm depth and 15 cm from the field edge, Acuros reports PD of 0.01%. For a 50 Gy treatment, the estimated dose to the fetus is 5 mGy. When using Table 1, PD was measured to 0.03% and the estimated dose would be 15 mGy. The average percent error from measured PD compared to Acuros for field sizes 3x3, 6x6, and 10x10 cm^2 at 15 cm from the field edge was -29%. It is highly

[a] Varian Medical Systems. (2014). Eclipse Photon and Electron Reference Guide

recommended that TPS calculated PD be verified by measurement when making critical clinical decisions on out of field OARs during treatment planning.

The Varian TrueBeam Representative Beam Data used for the models incorporates profiles that typically extend 5cm beyond the nominal field edge. This dataset was selected because it is widely available and frequently encountered in the clinical setting. It may be possible to improve agreement with measured doses by using a commissioning data set that extends further outside of the field edge and developing a beam model that uses parameters optimized for extra-focal radiation components. The manufacturer (Varian Medical Systems, Palo Alto, CA) was not able to clarify how much improvement could be expected if such an approach was used.

Neutron dose is also of concern when consider peripheral dose to electronic implantable devices, pediatric patients or fetus. The energies used in this paper do not exceed 10 MV; therefore, neutron dose is not expected contribute significantly to PD. In FFF beams, the absence of the flattening filter and reduced photon fluence is expected to reduce neutron contamination. We refer readers to the AAPM report on FFF beams for a detailed discussion on FFF beams and neutron dose[10].

5. CONCLUSIONS

Peripheral dose (PD) was measured for various field sizes (3 x 3- 30 x 30 cm^2) and distances from field edge (5 - 20 cm) for 6 FFF and 10 FFF beams in a solid water phantom. This comprehensive dataset can be used to estimate PD to out of field regions of interest such as organs at risk, electronic implantable devices, and the fetus. Peripheral dose was found to decrease with increasing energy and increase with increasing depth in the phantom. The impact of collimator rotation (0^o versus 90°) was found to slightly decrease PD; however, when combined with tertiary MLCs, the impact of collimator rotation was not clinically significant. Peripheral dose was calculated in a commercial treatment planning system using both AAA and Acuros dose calculation algorithms. Both algorithms underestimated the PD, and the magnitude of error varied with field size and distance from the field edge; therefore, physicists should use caution when interpreting and applying TPS calculated PD to determine dose to critical structures.

The authors have no relevant conflicts of interest to disclose

References

[1] F. Ponisch, U. Titt, O.N. Vassiliev, S.F. Kry, and R. Mohan, "Properties of unflattened photon beams shaped by a multileaf collimator," Med. Phys. **33**, 1738 - 1746 (2006).

[2] O.N. Vassiliev, U. Titt, S.F. Kry, F. Ponisch, M.T. Gillin, R. Mohan, "Monte Carlo study of photon fields from a flattening filter-free clinical accelerator," Med Phys **33**, 820-827 (2006).

[3] G. Kragl, S. af Wetterstedt, B. Knausl, M. Lind, P. McCavana, T. Knoos, B. McClean, and D. Georg, "Dosimetric characteristics of 6 and 10 MV unflattened photon beams," Radiotherapy and Oncology **93**, 141-146 (2009).

[4] G. Kragl, F. Baier, S. Lutz, D. Albrich, M. Dalaryd, B. Kroupa, T. Wiezorek, T. Knoos, and D. Georg, "Flattening filter free beams in SBRT and IMRT: Dosimetric assessment of peripheral doses," Z. Med. Phys. **21**, 91 - 101 (2011).

[5] S.F. Kry, O.N. Vassiliev, and R. Mohan, "Out-of-field photon dose following removal of the flattening filter from a medical accelerator," Physics in Medicine and Biology **55**, 2155-2166 (2010).

[6] D. Georg, T. Knoos, and B. McClean, "Current status and future perspective of flattening filter free photon beams," Med. Phys. **38**, 1280 - 1293 (2011).

[7] S.S. Almberg, J. Frengen, T. Lindmo, "Monte Carlo study of in-field and out-of-field dose distributions from a linear accelerator operating with and without a flattening-filter," Med Phys **39**, 5194-5203 (2012).

[8] K.H. Spruijt, M. Dahele, J.P. Cuijpers, M. Jeulink, D. Rietveld, B.J. Slotman, and W. Verbakel, "Flattening filter free vs flattened beams for breast irradiation," Int J Radiation Oncol Biol Phys **85**, 506 - 513 (2013).

[9] P. Tsiamas, J. Seco, Z. han, M. Bhagwat, J. Maddox, C. Kappos, K. Theodorou, M. Makrigiorgos, K. Marcus, and P. Zygmanski, "A modification of flattening filter free linac for IMRT," Med. Phys. **38**, 2342 - 2352 (2011).

[10] Y. Xiao, S.F. Kry, R. Popple, E. Yorke, N. Papanikolaou, S. Stathakis, P. Xia, S. Huq, J. Bayouth, J. Galvin, and F.F. Yin, "Flattening filter-free accelerators: a report from the AAPM therapy emerging technology assessment work group," Journal of Applied Clinical Medical Physics **16**, 12-29 (2015).

[11] J. Hrbacek, S. Lang, and S. Klock, "Commissioning of photon beams of a flattening filter-free linear accelerator and the accuracy of beam modeling using an anisotropic analytical algorithm," Int J Radiation Oncol Biol Phys **80**, 1228-1237 (2011).

[12] B.A. Fraass, J. van de Geijn, "Peripheral dose from megavolt beams," Med Phys **10**, 809-818 (1983).

[13] P.H. van der Giessen, and H.W.J. Bierhuizen, "Comparison of measured and calculated peripheral doses in patients undergoing radiation therapy," Radiotherapy and Oncology **42**, 265-270 (1997).

[14] M. Stovall, C.R. Blackwell, J. Cundiff, D.H. Novack, J.R. Palta, L.K. Wagner, E.W. Webster, R.J. Shalek, "Fetal dose from radiotherapy with photon beams: report of AAPM Radiation Therapy Committee Task Group No. 36," Med Phys **22**, 63-82 (1995).

[15] R.L. Stern, "Peripheral dose from a linear accelerator equipped with multileaf collimation," Med Phys **26**, 559-563 (1999).

[16] S. Mutic, J. Esthappan, E.E. Klein, "Peripheral dose distributions for a linear accelerator equipped with a secondary multileaf collimator and universal wedge," J Appl Clin Med Phys **3**, 302-309 (2002).

[17] A.N. Solan, M.J. Solan, G. Bednarz, and M.B. Goodkin, "Treatment of patients with cardiac pacemakers and implantable cadioverter-defibrillators during radiotherapy," Int J Radiation Oncol Biol Phys **59**, 897-904 (2004).

[18] R.M. Howell, S.B. Scarboro, S.F. Kry, D.Z. Yaldo, "Accuracy of out-of-field dose calculations by a commercial treatment planning system," Phys Med Biol **55**, 6999-7008 (2010).
[19] A. Fogliata, A. Clivio, E. Vanetti, G. Nicolini, M.F. Belosi, and L. Cozzi, "Dosimetric evaluation of photon dose calculation under jaw and MLC shielding," Med. Phys. **40**, 101706-101701 - 101712 (2013).
[20] S. Mutic, E.E. Klein, "A reduction in the AAPM TG-36 reported peripheral dose distributions with tertiary multileaf collimation. American Association of Physicists in Medicine Task Group 36," Int J Radiat Oncol Biol Phys **44**, 947-953 (1999).
[21] P.H. van der Giessen, "Calculation and measurement of the dose at points outside the primary beam for photon energies of 6, 10, and 23 MV," Int J Radiat Oncol Biol Phys **30**, 1239-1246 (1994).
[22] P.H. Van der Giessen, "A simple and generally applicable method to estimate the peripheral dose in radiation teletherapy with high energy x-rays or gamma radiation," Int J Radiat Oncol Biol Phys **35**, 1059-1068 (1996).
[23] S. Sherazi, K.R. Kase, "Measurements of dose from secondary radiation outside a treatment field: effects of wedges and blocks," Int J Radiat Oncol Biol Phys **11**, 2171-2176 (1985).
[24] K.R. Kase, G.K. Svensson, A.B. Wolbarst, M.A. Marks, "Measurements of dose from secondary radiation outside a treatment field," Int J Radiat Oncol Biol Phys **9**, 1177-1183 (1983).
[25] J.Y. Huang, D.S. Followill, X.A. Wang, S.F. Kry, "Accuracy and sources of error of out-of field dose calculations by a commercial treatment planning system for intensity-modulated radiation therapy treatments," J Appl Clin Med Phys **14**, 4139 (2013).
[26] A.M. Owrangi, D.A. Roberts, E.L. Covington, J.A. Hayman, K.M. Masi, C.I. Lee, J.M. Moran, and J.I. Prisciandaro, "Revisiting fetal dose during radiation therapy: Evaluating treatment techniques and a custom shield," Journal of Applied Clinical Medical Physics **Submitted**2015).
[27] Z. Chang, Q. Wu, J. Adamson, L. Ren, J. Bowsher, H. Yan, A. Thomas, F.-F. Yin, "Commissioning and dosimetric characteristics of TrueBeam system: Composite data of three TrueBeam machines," Medical Physics **39**, 6981-7018 (2012).
[28] M.L. Taylor, T. Kron, "Consideration of the radiation dose delivered away from the treatment field to patients in radiotherapy," Journal of Medical Physics / Association of Medical Physicists of India **36**, 59-71 (2011).